This is the published version of the publication, made available in accordance with the publisher's policy.

Slow oscillations open susceptible time windows for epileptic discharges

----

Sheybani, Laurent; Megevand, Pierre Bastien; Spinelli, Laurent; Bénar, Christian G.;
Momjian, Shahan Marc; Seeck, Margitta; Quairiaux, Charles; Kleinschmidt, Andréas Karl; Vulliemoz, Serge

Epilepsia®

Slow oscillations open susceptible time windows for epileptic discharges

Laurent Sheybani[1] | Pierre Mégevand[1,2] | Laurent Spinelli[1] |
Christian G. Bénar[3] | Shahan Momjian[4] | Margitta Seeck[1] | Charles Quairiaux[5] |
Andreas Kleinschmidt[1] | Serge Vulliémoz[1]

[1]EEG and Epilepsy Unit / Neurology, Department of Clinical Neuroscience, University Hospitals and Faculty of Medicine of University of Geneva, Geneva, Switzerland

[2]Department of Basic Neuroscience, Faculty of Medicine, University of Geneva, Geneva, Switzerland

[3]Aix-Marseille University, National Institute of Health and Medical Research, Institute of Systems Neurosciences, Marseille, France

[4]Neurosurgery, Department of Clinical Neuroscience, University Hospitals and Faculty of Medicine of University of Geneva, Geneva, Switzerland

[5]Functional Brain Mapping Laboratory, Department of Basic Neuroscience, Faculty of Medicine, University of Geneva, Geneva, Switzerland

Correspondence
Laurent Sheybani, Clinique de Neurologie, Département des Neurosciences Cliniques, Hôpitaux Universitaires de Genève, Genève, Switzerland.
Email: laurent.sheybani@unige.ch

Funding information
SCALES, Grant/Award Number: SCALES FLAG-ERA-JTC2017; Schweizerischer Nationalfonds zur Förderung der Wissenschaftlichen Forschung, Grant/Award Number: 167836, 192749, CRSII5 170873, 163398 and CRS115-180365; Interne Scientifique position, University Hospital of Geneva, Grant/Award Number: n.a.

Abstract

Objective: In patients with epilepsy, interictal epileptic discharges are a diagnostic hallmark of epilepsy and represent abnormal, so-called "irritative" activity that disrupts normal cognitive functions. Despite their clinical relevance, their mechanisms of generation remain poorly understood. It is assumed that brain activity switches abruptly, unpredictably, and supposedly randomly to these epileptic transients. We aim to study the period preceding these epileptic discharges, to extract potential proepileptogenic mechanisms supporting their expression.

Methods: We used multisite intracortical recordings from patients who underwent intracranial monitoring for refractory epilepsy, the majority of whom had a mesial temporal lobe seizure onset zone. Our objective was to evaluate the existence of proepileptogenic windows before interictal epileptic discharges. We tested whether the amplitude and phase synchronization of slow oscillations (.5–4 Hz and 4–7 Hz) increase before epileptic discharges and whether the latter are phase-locked to slow oscillations. Then, we tested whether the phase-locking of neuronal activity (assessed by high-gamma activity, 60–160 Hz) to slow oscillations increases before epileptic discharges to provide a potential mechanism linking slow oscillations to interictal activities.

Results: Changes in widespread slow oscillations anticipate upcoming epileptic discharges. The network extends beyond the irritative zone, but the increase in amplitude and phase synchronization is rather specific to the irritative zone. In contrast, epileptic discharges are phase-locked to widespread slow oscillations and the degree of phase-locking tends to be higher outside the irritative zone. Then, within the irritative zone only, we observe an increased coupling between slow oscillations and neuronal discharges before epileptic discharges.

Significance: Our results show that epileptic discharges occur during vulnerable time windows set up by a specific phase of slow oscillations. The specificity of these permissive windows is further reinforced by the increased coupling of neuronal activity to slow oscillations. These findings contribute to our understanding

of epilepsy as a distributed oscillopathy and open avenues for future neuromodulation strategies aiming at disrupting proepileptic mechanisms.

KEYWORDS

human epilepsy, interictal epileptic discharges, intracranial recording, phase–amplitude coupling, slow oscillations

1 | INTRODUCTION

Interictal epileptic discharges (IEDs) are a diagnostic hallmark of epilepsy[1] and a valuable feature for delineating the seizure onset zone (SOZ) in presurgical evaluation of epilepsy.[2] They have been shown to promote,[3] or at least modulate,[4] the process of epileptogenesis. Furthermore, they may contribute to the various cognitive comorbidities in patients with epilepsy.[5] Despite this broad relevance for patients suffering from epilepsy, we currently have only a sparse knowledge of the mechanisms supporting their expression. The identification of a pattern of activity occurring specifically before IEDs is a necessary step to elucidate these proepileptogenic mechanisms.

The current understanding of IEDs is that they arise from synchronous and rhythmical discharges of a population of neurons.[6] One putative mechanism by which neurons could synchronize their discharges lies in synchronization of ongoing membrane potential fluctuations. Low-frequency oscillations are considered to support the interaction between different brain regions by aligning the excitability windows of individual neurons.[7,8] Along the same lines, we showed in previous work on the epileptic mouse model of hippocampal sclerosis that fast ripples in neocortical regions are phase-locked to 3–5-Hz oscillations.[9] Another supporting piece of evidence comes from human neuronal activity during sleep. It is modulated by slow waves of <4 Hz,[10] and IEDs occur preferentially at the transition between the up and down states of .5–1-Hz sleep slow waves.[11] On a larger timescale, the identification of cyclic multidien patterns of occurrence of epileptic seizures and IEDs[12,13] supports the existence of recurring permissive windows in the emergence of epileptic activity. These permissive windows could be related to the co-occurrence of IEDs and sleep slow waves,[11] the latter modulating neuronal discharges in physiological conditions.[10] In epilepsy, evidence exists that the modulation of high-frequency oscillations (80–150 for ripples and >200 Hz for fast ripples in Ibrahim et al[14]) and neuronal activity (estimated by high-gamma activity [80–150 Hz][15]) by a slower oscillatory activity can help to localize the SOZ, through either a strengthened modulation within the SOZ[14–16] or a modulation on a slightly different phase of slow oscillations

Key Points

- There is growing evidence that pathological rhythms modulate the expression of IEDs
- We used human intracranial recordings with focal refractory epilepsy to study oscillatory changes anticipating the expression of IEDs
- A large-scale network of SOs sets a permissive milieu for IED expression
- Coupling between SOs and neuronal activity increases directly before IEDs, making it a strong proepileptogenic mechanism candidate

(SOs) within the SOZ.[17] It is also known that gamma activity (30–100 Hz) increases before IEDs,[18] but it remains unclear whether pathological modulations by SOs exist, and whether the modulation of neuronal activity by SOs is specific to the period preceding IED occurrence. The lack of evidence could be because the firing pattern of neurons before IEDs is highly heterogeneous.[19,20]

Our working hypothesis is that widespread changes in coordination of SOs generate a permissive background from which IEDs emerge as a pathological transient. We address these changes by analyzing, in the period preceding the IED, the time course of amplitude and cross-regional synchronization of SOs as well as their phase-locking to the upcoming IED. To further explore the relation between SOs and neuronal activity, we also investigate the relationship between the ongoing phase of SOs and neuronal activity in the time windows immediately leading up to the IED. We test this by measuring the coupling of the SOs phase to high-gamma band activity, as a surrogate marker of neuronal activity.[15,21]

2 | MATERIALS AND METHODS

2.1 | Patients

Ten patients (three female) were included in the study (Table S1). They all underwent intracranial

electroencephalographic (EEG) monitoring for intractable focal epilepsy at the Epilepsy Unit of Geneva University Hospital. Mean age at recording was 37 years (range = 21–53), mean age at onset of epilepsy was 23.5 years (range = 9–40), and mean duration of epilepsy was 13.5 years (range = 3–31). Table S1 gives an overview of the patients' clinical data. The study was approved by the local ethical committee (Commission Cantonale d'Ethique de la Recherche, Canton de Genève, Switzerland, protocol #13-004), and patients gave written informed consent to participate in the study.

2.2 | Acquisition and organization of data

Between 6 and 18 depth electrodes per patient were implanted stereotactically (DIXI medical and Ad-Tech electrodes). Each electrode contained between five and 18 recording contacts along the shaft, providing a total of 1278 recording contacts. Data were acquired with SystemPlus Evolution Micromed at a sampling frequency of 2048 Hz and resampled offline (linear interpolation to 1000 Hz). All analyses were then performed with a bipolar montage.

The anatomical localization of recording contacts was visually identified in Cartool software[22] after coregistration of a postoperative submillimetric computed tomographic image with the preoperative T1 magnetic resonance imaging (MRI; Analyze software, Biomedical Imaging Resource, Mayo Clinic; see an example in Figure S1). We visually grouped contacts based on their anatomical location into "regions" or "brain regions" and excluded from analysis contacts located in white matter or outside the brain.

The current dataset also included simultaneous high-density scalp EEG (256 recording channels, Electrical Geodesics, sampling frequency = 1000 Hz). In this study, we only used scalp EEG to identify slow wave sleep versus awake state (background slowing, spindles, K-complexes). Non-rapid eye movement sleep Stages 2 or 3 were absent ($n = 8$) or rare ($n = 2$) in our patients.

2.3 | Identification of IEDs and baseline markers in data

A board-certified epileptologist (S.V.) visually identified a total of 1074 IEDs following the definition by Kural et al.[23] and classified them for further analysis into 35 IED types according to their location, morphology, and polarity (Figure S2). The majority of IEDs were recorded in temporomesial structures, and all others also involved the limbic system. One single marker was attributed to each IED, whether it occurred on one or more than one channel. The number of IEDs per IED type ranges from three to 156 (see Figure S2). We included either epileptic spikes (<70 ms) or sharp-wave discharges (70–200 ms). Slow rhythmic or periodic pattern and fast epileptic activity were not included.[24] A typical example can be seen in Figure S5. From this visual classification, we obtained 548 IEDs from left hippocampus, 123 from left amygdala, 28 from left insula, 342 from right hippocampus, and 33 from right cingulate cortex. We then automatically identified the positive or negative peak of IEDs to align pre-IED windows of interest. IEDs marked within 2000 ms after a given IED were not considered. For control purposes, we generated random markers within the timeframes of each respective EEG duration, and then discarded all baseline markers that occurred either ±2000 ms around an IED, or in the 2000 ms that followed another baseline marker. Time windows for statistical analyses spanned from −1250 to −250 ms before IEDs' markers (see Figure S3 and below), whereas time windows used to filter the data spanned from −6000 ms to 6000 ms around IEDs.

2.4 | Management of spectral leakage of IEDs

Spectral leakage refers to the finding that the activity within one frequency range can contaminate the frequency content of virtually all other frequency bands,[25] which can be problematic when measuring slow activity locked to IEDs.[25] We thus took two conservative measures to prevent the energy of the IEDs from leaking into slower frequencies. First, we stopped the statistical analysis of SOs at −250 ms before IEDs peak using an automated detection (>90% of IEDs have a statistical onset after this boundary; statistical onset as described in Sheybani et al.[26] and shown in Figure S3). This 250-ms buffer strongly limits the possibility that backward leakage of spectral energy from the IED contaminated our analyses. The second measure was to analyze data using three different filtering methods: (1) a zero-phase digital filter ("classical" filter), and two complementary methods: (2) a one-dimensional digital forward filter ("forward" filter, Figure S4), which prevents the IED itself from leaking over the pre-IED period (but leads also to phase distortion, see Supporting Information); and (3) a "classical" filter (Figure S5), with the concatenation of the EEG epoch from −6000 to −250 ms before the IED and the same activity, but inverted in the time domain to suppress the IED from the analyzed window. For clarity, only the results of the classical filter are

shown (but statistical analyses are applied to the three methods). We interpreted results as (1) statistically confirmed if the three filtering methods yielded significant results, (2) probable if two filtering methods yielded significant results, (3) possible if one filtering method yielded significant results, and (4) nonexistent if no filtering method yielded significant results. Finally, to prevent edge effect, we adapted the window for statistical analysis (−1250 to −250 ms) on only a small portion of the windows used to filter data (−6000 to 6000 ms).

2.5 | Frequency analyses

2.5.1 | Pre-IED analyses: Amplitude, phase-locking, and phase synchronization

Pre-IED activity (−1250 to −250 ms) was analyzed individually for each contact and IED. Data were filtered within .5–4 Hz and 4–7 Hz after initial analyses revealed that amplitude in both frequency ranges increases before IEDs (see Figure 1). SOs usually encompass the frequency range of <4 Hz,[10] but the term has also been used to define oscillations up to 6 Hz.[27] Thus, for the sake of clarity, we used the term SO for both .5–4-Hz and 4–7-Hz frequency ranges. Filtered data were Hilbert-transformed using the function *hilbert* in MATLAB (MathWorks), to extract the instantaneous amplitude and phase. The phase-locking of IEDs to SOs was obtained through the intertrial coherence (ITC),[28] defined as:

$$ITC = \frac{1}{N} \left| \sum_{k=1}^{N} e^{i * \varphi k} \right|$$

where N is the number of IEDs within one IED type, k is the current epoch (i.e., IED), and φ is the phase of the signal. ITC was used (1) across trials and within contacts to determine phase locking and (2) within trials and across contacts (i.e., across the difference of phase of two contacts using the toolbox *CircStat*[29]) to detect synchronization.

2.5.2 | Phase–amplitude coupling

Phase–amplitude coupling between the phase of SOs and the amplitude of high gamma, a proxy for neuronal activity,[15,21] was quantified by the modulation index, following the procedure described in Tort et al.[30] and implemented in *ft_crossfrequencyanalysis* of the Fieldtrip toolbox.[31] To include at least one complete period of oscillation within the 1-s window of analysis, we used here a slightly different frequency range (1–4 Hz instead of .5–4 Hz).

The analysis pipeline is further described in Figure S7.

2.5.3 | Operational definition of the irritative zone

To evaluate the spatial specificity of our observations (inside vs. outside the irritative zone [IZ]), we had to select an operational definition of the IZ. In most analyses, we used an objective threshold detection based on the increase of amplitude within the frequency range of IEDs (20–30 Hz). For the analysis of phase-locking in regions outside the IZ (Figure S6), we used a more restrictive definition based on visual identification of the IZ. Further information about the definition of the IZ can be found in the Supporting Information.

## 2.6 | Statistical information

We calculated the ratio of each measure during the pre-IED condition divided by baseline condition (amplitude, synchronization, phase-locking, and phase–amplitude coupling). According to the null hypothesis, this ratio is equal to 1 (no difference between baseline and pre-IED period). We then calculated the average of each variable for regions outside and inside the IZ across each patient. We obtained one value per patient (and for each of the four conditions) that we used to compute the statistics, thus using each patient as an independent variable. We used a paired, nonparametric test (Friedman test) and Dunn corrections for multiple comparisons within the software Prism (GraphPad Software). The alpha threshold was set at .05. As we used three different filtering methods, we considered that results confirmed by the three filters were statistically significant, those confirmed by two filters were "probable," and those confirmed by only one filter were "possible." To correct for multiple comparisons of IED amplitude (for the identification of IZ regions), we used the Sidak correction. Analyses were performed in MATLAB, Fieldtrip,[31] and Prism.

3 | RESULTS

3.1 | Characterization of brain activity preceding IEDs across brain regions

We first investigated patterns of signal changes surrounding the IED by averaging signals in the time domain ±1500 ms around each IED. Each of the 10 patients expressed specific IED types (defined by their morphology, polarity, and location), and the number of IED types per patient varies between two and five (Figure S2). After
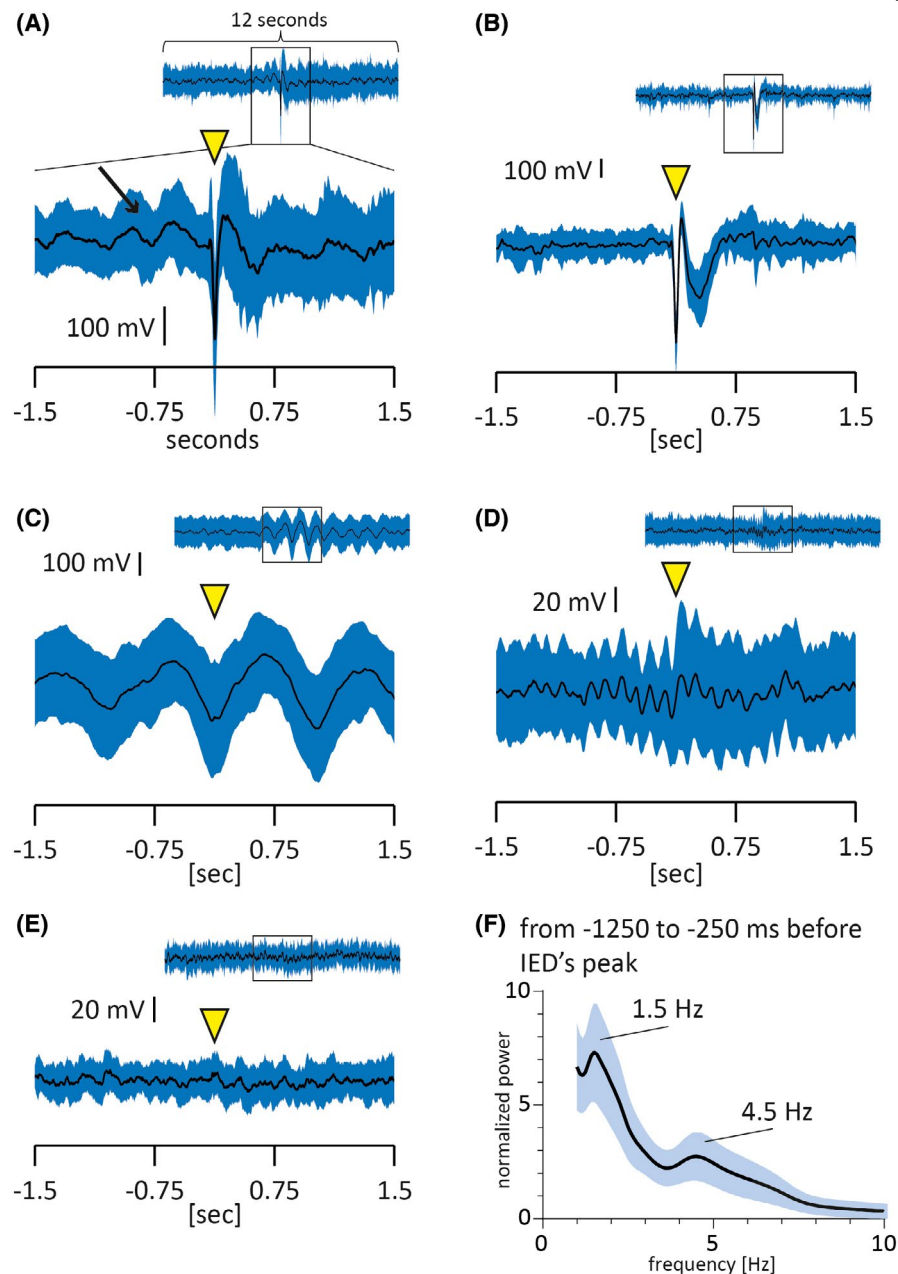
FIGURE 1 Characterization of brain activity before interictal epileptic discharges (IEDs) across brain regions. (A–E) Averages of multiple IED epochs, centered on IED peak, showing contacts simultaneously recording an IED (A, B) or not (C–E). Average raw signal ± SD across the repetitions of one IED type is shown. For each panel in A–E, the number of IED epochs to obtain the depicted average is indicated (*n*); the *n* is not always the same, as these examples are not always taken from the same IED type. Each window lasts 3 s and is taken from the black square in the miniature average inserted at the top right of each panel. The peak of the IED is marked in the trace of the contact recording the IEDs to align all other contacts (yellow arrowhead). (A) Some contacts show a clear peak time-locked to the IED and also a slow oscillation (SO; delta, .5–4 Hz, black arrow) preceding the actual IED (*n* = 91). (B) Other contacts record the IED but no detectable SO (*n* = 26). (C) Yet other contacts show an SO locked to the IED peak, but no sharp transient activity (i.e., no activity within the frequency range of the IED; *n* = 91). (D, E) In some contacts, the preceding SO is slightly faster (D; theta, 4–7 Hz; *n* = 75), and finally, the remaining contacts show neither an activity within the range of the IED nor an SO (E; *n* = 28). (F) The grand average normalized spectrogram (*z*-score ± SEM against baseline epochs free of IED) across all patients and all IED types over the pre-IED period (−1250 to −250 ms before IED peak) shows a peak at 1.5 Hz and 4.5 Hz concordant with the findings in A, C, and D (*n* = 1074)

averaging across IEDs of the same type, some contacts reveal a transient sharp event (the IED), and a surrounding SO in the delta range (.5–4 Hz; Figure 1A). Other

contacts show only the averaged IED without surrounding SOs (Figure 1B). Further contacts contain no central peak, indicating that these contacts are probably located

outside the IZ, and only show an SO in the delta range (.5–4 Hz; Figure 1C) or theta range (4–7 Hz; Figure 1D). Finally, the last type of contact does not show any time-locked activity (Figure 1E). The average, normalized (i.e., *z*-scored against baseline) spectrogram across contacts inside the IZ (i.e., contacts recording an IED) and across IED types shows peaks at 1.5 Hz and 4.5 Hz before the IED itself (from −1250 to −250 ms; Figure 1F). To further explore the pre-IED period, we proceeded to an IED-by-IED analysis of SO activity.

3.2 | Amplitude of SOs increases before IEDs, with spatial selectivity for IZ

After filtering the data in the frequency bands of interest (Figure 2A,B), we obtained the amplitude (Figure 2C–E) and ITC (Figure 2F-H) within 12-s time windows. In this example, the amplitude of SOs (here, .5–4 Hz) increases before the IED (Figure 2D; mean $\pm$ SD across the repetition of one representative IED type), whereas no variation is seen during baseline activity (Figure 2E).

Statistical analysis reveals a significant amplitude increase of SOs in the pre-IED period, with a specificity for the IZ. Inside the IZ, we observed a significant amplitude increase for the frequency range 4–7 Hz (median increase = +14.1%, $p = .006$; see Figure 3 for details of statistical analyses and results), and a probable increase for the range .5–4 Hz (statistically confirmed by two filters, median increase = +10.4%, $p = .008$; Figure 3A; see Materials and Methods for the definition of "significant," "probable," and "possible"). On the other hand, for regions outside the IZ, we observed only a possible increase for the range .5–4 Hz (statistically confirmed by one filter, median increase = +4.1%, $p = .04$) and no increase for the range 4–7 Hz (Figure 3A).

3.3 | Brain regions synchronize before IEDs, with spatial selectivity for IZ

To test whether phase synchronization between contacts increases before an IED, we calculated the ITC of the difference of phase across time between pairs of contacts. Similar to the analysis of amplitude, we observed a significant increase in synchronization, with a specificity for the IZ. The increase in synchronization across the different filters and both frequency ranges is significant for regions inside the IZ (median increase = +.9–1.9%, $p < .05$; Figure 3B; see Figure 3 for details of statistical analyses and results). Outside the IZ, there is only a probable increase for the frequency range .5–4 Hz (statistically confirmed by two filters, median

increase = +.8%, $p = .005$), and there is no increase for the frequency range 4–7 Hz (Figure 3B).

3.4 | IEDs are phase-locked to SOs, including those recorded outside IZ

In Figure 2F–H, we illustrate the evolution of ITC around IEDs, which assesses whether there is an alignment of ongoing oscillation phase before IEDs. In this example (Patient P03), we observed an ITC increase before IEDs (Figure 2G), whereas ITC remained low during baseline (Figure 2H). This alignment indicates that IEDs are phase-locked to ongoing SOs. As further shown in Figure 4A, we display eight single traces, the alignment of which anticipates IED peak by around 1000 ms. The circular plots above indicate the phase angle of the eight signals at −3500 ms, −2500 ms, and −750 ms. Phases are more aligned at −750 ms than at earlier time points. This phase concentration is reliably quantified by the ITC (Figure 4B). Of note, that we measured ITC over a long time window (1 s) implies that IEDs are phase-locked to oscillations of the same frequency, and not only to a common phase (Figure 4A,C).

The same analyses across all contacts and IED types show that phase-locking of IEDs to SOs is significant in regions outside the IZ for both frequency ranges (median increase = +97–115%, $p < .05$; Figure 3C; see Figure 3 for details of statistical analyses and results). In regions inside the IZ, there is a probable phase-locking to .5–4 Hz (statistically confirmed by two filtering methods, median increase = +91%, $p = .01$) and possible phase-locking to 4–7 Hz (statistically confirmed by one filtering method, median increase = +74%, $p = .049$; Figure 3C).

Although there is no significant difference between the phase-locking of regions inside versus outside the IZ for the frequency range .5–4 Hz, the systematically significant phase-locking to SOs recorded outside the IZ is intriguing. This means that IEDs might be phase-locked to a large-scale network of SOs. To further spatially dissect this observation, we analyzed data on a region-by-region basis to find out which regions outside the IZ show a significant increase in ITC and whether these regions present a systematic increase in ITC across IED types (and thus patients; Figure S6). Significant ITC increases were found in all patients but one. Regarding regions, the increase in phase-locking occurs in numerous regions, but the extent of increased ITC is heterogeneous and not confined to the hemisphere ipsilateral to the IZ. Nonetheless, the most systematic increase in phase-locking across IED types was found in the ipsilateral lateral temporal region, ipsilateral insula, ipsilateral dorsolateral prefrontal region, and contralateral lateral temporal region.
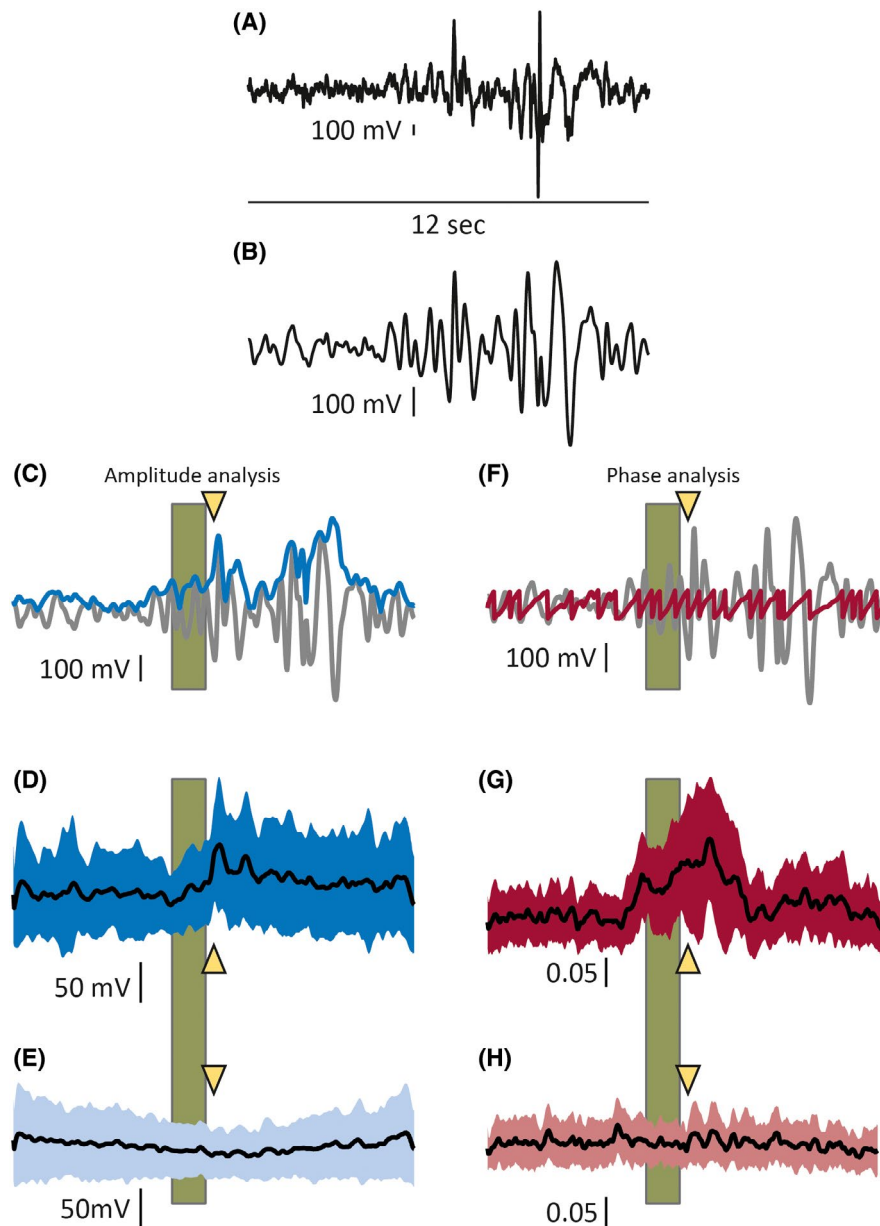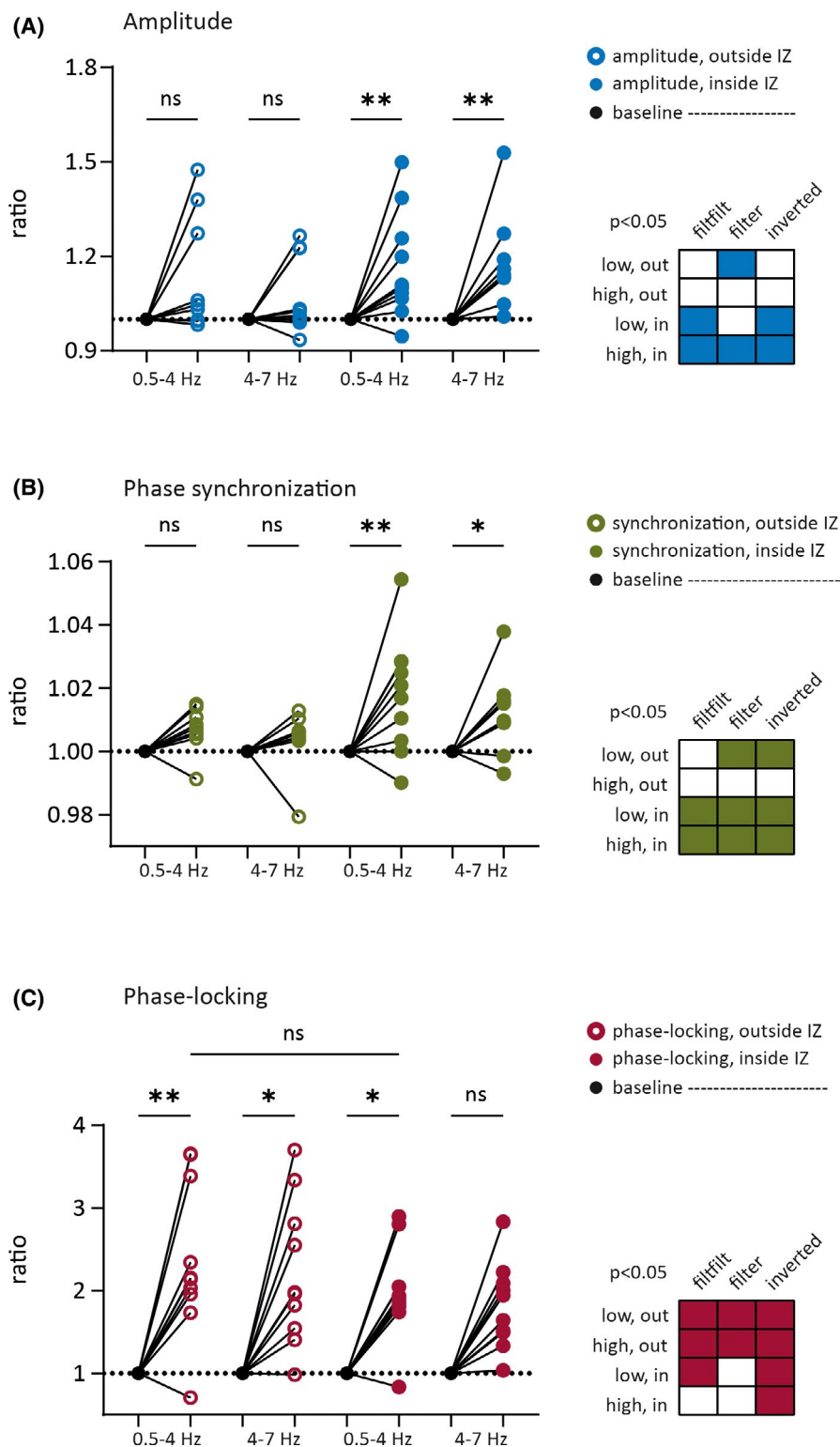
FIGURE 2 Data analysis procedure for amplitude and phase analyses, locked to interictal epileptic discharge (IED) peak. The same procedure was applied with all three filters ("classical," "forward," "inverted") and within two different frequency bands (.5–4 Hz and 4–7 Hz). (A) Raw data: example of a single 12-s window in one contact centered on a detected IED. (B) Filtered data; each window is processed individually. In the first step, data are bandpass filtered between .5–4 Hz and 4–7 Hz. (C) The amplitude of the filtered data is then obtained using the absolute values of the Hilbert transform. The process is repeated across all detected IEDs. The gray line indicates the filtered data (as in B) and the blue line the extracted amplitude. (D) Mean ± SD of the amplitude for a single contact across repeated IEDs ($n = 91$). (E) Same as D, but locked to control markers during baseline. (F) The phase of the filtered data is obtained using the phase of the Hilbert transform. This process is repeated across all detected IEDs. Intertrial coherence (ITC) is calculated across the repetition of IEDs for every single contact. The gray line indicates the filtered data (as in B and C) and the red line the extracted phase. (G) Mean ± SD of ITC across contacts ($n = 156$), locked to the detected IEDs. (H) Mean ± SD of ITC across contacts, locked to baseline markers. Bronze rectangles indicate the window for statistical analysis (i.e., −1250 ms to −250 ms before the IED peak)

3.5 | Phase–amplitude coupling between SOs and neuronal activity (high gamma) increases before IEDs, with spatial selectivity for IZ

We then looked, inside the IZ, for a local correlate of the link between SOs and ongoing neuronal activity, which

might eventually transform into the emergence of an IED. To this end, we used phase–amplitude coupling between high-gamma activity, a proxy of neuronal activity[15,21] and SOs. We found two peaks in the high-gamma range in the 1 s preceding the IEDs (Figure 5A, top). They occur around 400 ms apart and also translate into the average z-score (Figure 5A, middle), whereas this

(A) Amplitude

- ○ amplitude, outside IZ
- ● amplitude, inside IZ
- ● baseline ----------------

(B) Phase synchronization

- ○ synchronization, outside IZ
- ● synchronization, inside IZ
- ● baseline ----------------------

(C) Phase-locking

- ○ phase-locking, outside IZ
- ● phase-locking, inside IZ
- ● baseline ----------------------

modulation is not seen for lower frequencies (1–50 Hz; Figure 5A, bottom). In other words, high-gamma activity is modulated at around 2.5 Hz in the 1 s that precedes the IED. We then studied the coupling between delta phase (i.e., 1–4 Hz; see Materials and Methods) and high-gamma amplitude (60–160 Hz). Across IED types, we observed a significant increase in phase–amplitude coupling before IEDs for regions inside the IZ (median increase = +1.4%, p = .007; see Figure 5 for details of statistical analyses and results), whereas no significant difference was observed for regions outside the IZ (Figure 5B), confirming that the pre-IED amplitude of high-gamma activity is modulated by an SO in the 1–4-Hz range within the IZ.

FIGURE 3 Before interictal epileptic discharges (IEDs), amplitude and phase synchronization increase inside the irritative zone (IZ), whereas phase-locking involves a wider network. For clarity, only results with the classical filter are displayed here. The 4×3 chessboard at the bottom right of each panel gives a synopsis of statistical analyses across filtering methods. The square is white when the analysis is nonsignificant and colored when it is significant; "low" and "high" indicate the ranges .5–4 Hz and 4–7 Hz, respectively; "out" and "in" indicate regions outside and inside the IZ, respectively. Colored circles and full disks indicate results for regions outside and inside the IZ, respectively. Black full disks indicate baseline epochs. (A) Amplitude increases significantly for the frequency range 4–7 Hz in regions inside the IZ (median increase = +14.1%, interquartile range [IQR] = 3.8%–21%, $p = .006$), but not outside the IZ. Amplitude increases probably for the frequency range .5–4 Hz in regions inside the IZ (median = +10.4%, IQR = 5.6%–28.9%, $p = .008$) but only possibly for regions outside the IZ (median = +4.1%, IQR = .5%–26.7%, $p = .04$). (B) Phase synchronization during the same time window increases significantly for both frequency ranges in regions inside the IZ (.5–4 Hz: median = +1.9%, IQR = .3%–2.8%, $p = .002$; 4–7 Hz: median = +.9%, IQR = .6%–1.7%, $p = .01$). Furthermore, synchronization increases probably for the frequency range .5–4 Hz for regions outside the IZ (median = +.8%, IQR = .6%–1.2%, $p = .005$). There is no increase for the frequency range 4–7 Hz for the regions outside the IZ. (C) IEDs are phase-locked to oscillations recorded outside of the IZ for the frequency range .5–4 Hz (median = +115%, IQR = 90%–245%, $p = .002$) and 4–7 Hz (median = +97%, IQR = 51%–194%, $p = .01$). IEDs are probably phase-locked to oscillations recorded inside the IZ for the frequency range .5–4 Hz (median = +91%, IQR = 79%–124%, $p = .01$) and only possibly for the frequency range 4–7 Hz (median = +74%, IQR = 44%–121%, $p = .049$). Each aligned dot plot shows the increase of each variable (amplitude, synchronization, and phase-locking) for each of the 10 patients. We used a nonparametric Friedman test with Dunn correction for multiple comparisons; $n = 10$ patients in each condition. Probability values displayed are calculated after correction for multiple comparisons. "Probable" indicates that the effect is statistically confirmed by two filtering methods; "possible" indicates that the effect is statistically confirmed by one filtering method. *$p < .05$, **$p < .01$; ns, not significant

It is important to recall that the 2 s preceding IEDs in our analyses are, by construction, void of other IEDs (see Materials and Methods). Therefore, contamination by preceding IEDs (or systematic spiky artifact) cannot account for this phase-modulated high-gamma activity.

4 | DISCUSSION

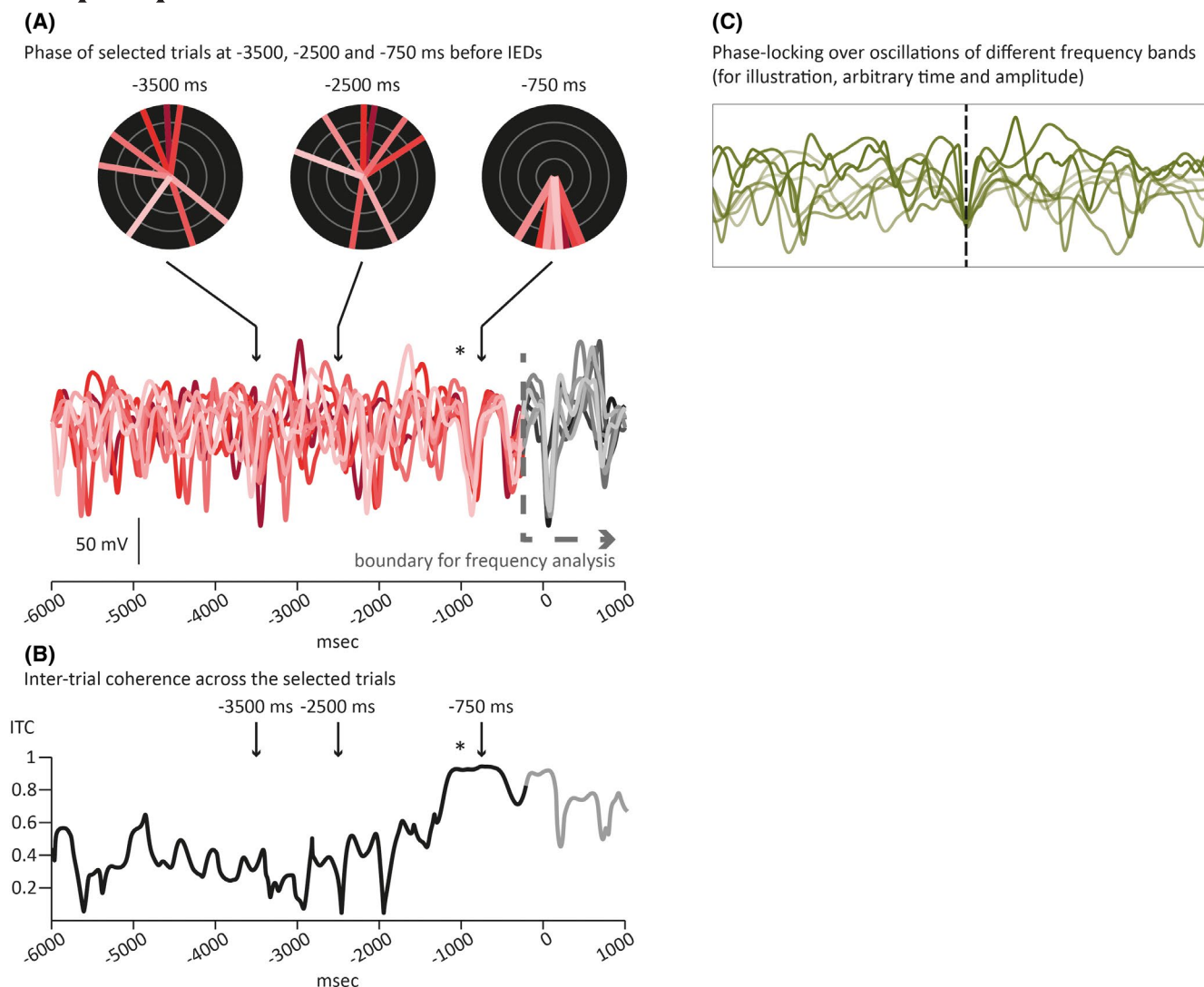## 4.1 | Deciphering neural syntax leading up to interictal epileptic discharges: Therapeutic perspectives

IEDs have a broad relevance, from both clinical and research perspectives. They are helpful markers in presurgical evaluation of epilepsy, as they can estimate the SOZ.[2] They are also known to disrupt—at least transitorily—normal cognitive function and memory in particular.[5] Furthermore, some evidence supports their role in epileptogenesis.[3] They should thus represent priority targets for the development of future treatments. Innovative closed-loop neuromodulation protocols that could predict their occurrence and selectively prevent their expression are an attractive perspective.[32] These protocols will need to be informed with a precise understanding of the activity preceding IEDs, to predict them with high reliability. Complementarily, the development of new medications is strongly dependent on a better knowledge of the mechanisms underlying the emergence of IEDs. In the present study, we tackled both aspects; we tested the hypothesis that identifiable pathological rhythms in the slow oscillatory range anticipate upcoming IEDs, and we provided a potential mechanistic link between SOs and emergence of

IEDs, that is, phase–amplitude coupling of high-gamma activity to SOs.

The phase-locking of IEDs to SOs reveals that IEDs occur at a specific phase of SOs that could be understood as vulnerable windows of excitability for IED expression. Within these windows of excitability, we observed an increased amplitude and phase synchronization, which are both spatially tied to the IZ. Comparatively, in physiological conditions, the phase of oscillations can dictate the conscious perception of audiovisual stimuli[33]; on the network level, the interaction between brain regions relies, at least in part, on the synchronization of their activity by oscillations,[7,8] which allows integration of the activity of spatially distant neuronal populations involved in a common task.[7] These findings suggest that changes in a large-scale SO network build up a favorable context for the emergence of IEDs. Although formal demonstration of causality requires a manipulation of the network, we nevertheless wanted to identify a local correlate of the link between SOs and IEDs. Locally, we thus provide a candidate mechanism supporting the emergence of IEDs during the increased slow oscillatory background: an enhanced phase–amplitude coupling of neuronal discharges to SOs. Such coding of neuronal activity along the phase of a slower oscillation is a type of neural syntax known to subserve cognitive processes.[30] Interestingly, in epilepsy, using such coding to predict upcoming seizures has been shown to improve predictive algorithms.[34]

Our findings dovetail nicely with the work by Frauscher and colleagues, who showed that IEDs preferentially occur during slow waves of sleep, and more specifically at the transition from "up" to "down" states.[11] These slow waves are known to modulate neuronal activity,[10] but the

(A)

Phase of selected trials at -3500, -2500 and -750 ms before IEDs

(C)

Phase-locking over oscillations of different frequency bands (for illustration, arbitrary time and amplitude)

(B)

Inter-trial coherence across the selected trials

FIGURE 4 Ongoing oscillations align before interictal epileptic discharges (IEDs), as measured by the intertrial coherence (ITC). (A) Representative example of signal alignment across eight trials. Each trial is depicted by the different intensity of red. At −3500 and −2500 ms before the IED, the phases are dispersed across the different trials, but starting ~1000 ms (*) before the IED, signal aligns across trials such that the phase of the eight trials converges toward one angle (as shown in the circular plots above). (B) ITC reliably reflects this alignment across trials with a corresponding increase. When ITC is calculated on the superposition of different trials from the same contact, it thus identifies periods of phase-locking. Comparatively, when ITC is calculated on the difference of phase between two signals across time, it thus identifies the synchronization between these two signals. (C) The green traces were created for illustration and do not represent actual data. Here, in contrast with A, where oscillations align with each other, the green traces in C align only to the timepoint of interest (dashed vertical line), which indicates a phase-locking of oscillations that belong to different frequency bands (around the dashed vertical line, oscillations are not superimposed, as they are in A). Thus, the use of ITC over 1-s windows shows that phase-locking of IEDs is phase- and frequency-dependent

link with the expression of epileptic discharges had not been reported so far.

## 4.2 | Modulation of activity of IZ by extra-IZ oscillations

The phase-locking of IEDs to extra-IZ oscillations was systematically observed across the three filtering methods. This is in line with several observations that the occurrence of IEDs is related to cortical activity within a large-scale epileptic network.[35] Regarding seizures, regions involved in the generation of ictal activity can extend beyond the structural lesion identified on MRI in patients with focal epilepsy due to focal cortical dysplasia.[36] Moreover, several studies have shown that activity in regions remote from the SOZ can modulate its activity,[37,38] and conversely IEDs can induce spindles
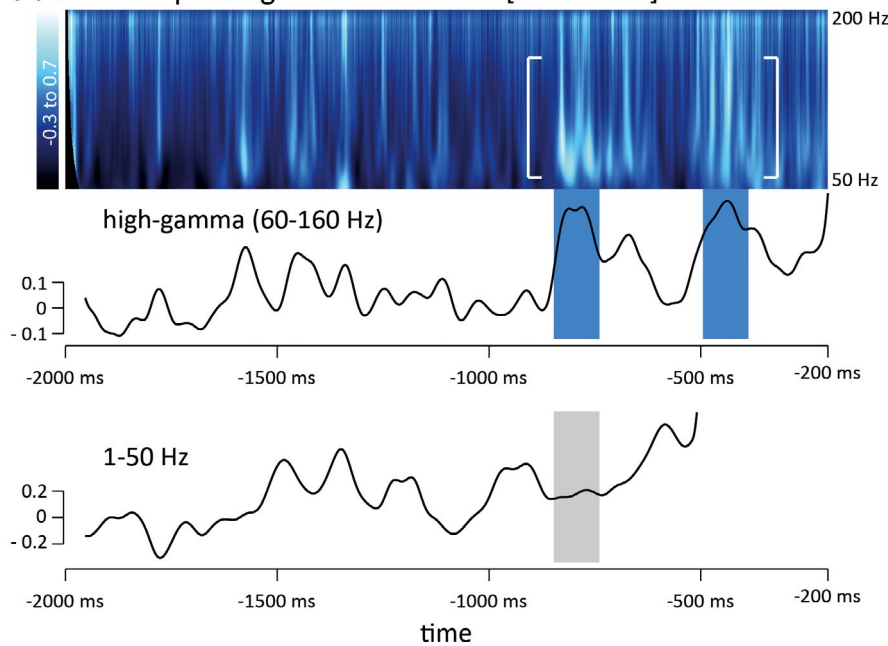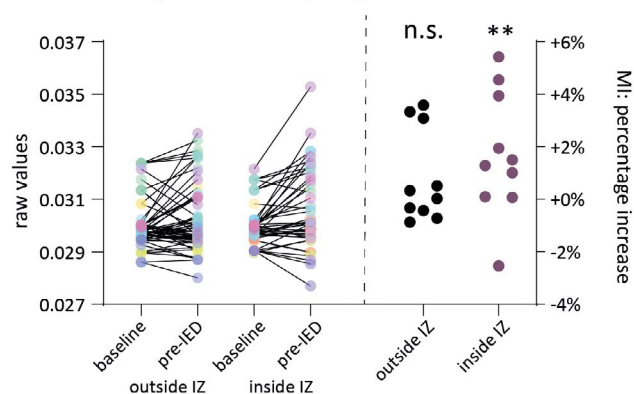
FIGURE 5 Phase–amplitude coupling between slow oscillations and neuronal activity (high gamma) increases before interictal epileptic discharges (IEDs). (A) Illustration of phase–amplitude coupling. Top: Normalized time–frequency activity (z-score) shows two periods of increased amplitude at 60–160 Hz (between white square brackets). Middle: Average of the normalized time–frequency activity (z-score). A phase–amplitude coupling should show a periodic increase of high-gamma activity along the phase of slower frequency activity. Here, the two periods of increased amplitude in the last 1 s of the plot, ~400–500 ms apart (blue rectangles), suggest a modulation of high-gamma activity by an underlying 2–3-Hz oscillation. Bottom: The normalized spectrogram for 1–50 Hz does not show such a pattern of amplitude modulation (notably no peak simultaneous to the first peak of high-gamma amplitude, gray rectangle), confirming that the modulation of amplitude is specific for the high-gamma activity (the normalized 1–50-Hz spectrogram is truncated at −500 ms because of the subsequent high increase in amplitude that would artificially flatten the preceding activity). (B) Pre-IED phase–amplitude coupling (−1250 to −250 ms) between the phase of the 1–4-Hz oscillation and the amplitude of 60–160-Hz activity, compared to the baseline period. On the left of the dashed bar, we display the raw modulation index of regions outside the irritative zone (IZ; first two left dots) and inside the IZ (last two right dots). Each color corresponds to one patient (each patient has >1 dot, as each patient has >1 IED type). On the right of the dashed bar, we display the effect sizes for regions outside the IZ (black dots) and inside the IZ (purple dots). There is a significant pre-IED increase in regions inside the IZ (median = +1.4%, interquartile range [IQR] = .1%–4.1%, $p = .007$), but no difference for regions outside the IZ (median = +.2%, IQR = −.005%–3.2%). We used a nonparametric Friedman test with Dunn correction for multiple comparisons; $n = 10$ patients. Probability value after correction for multiple comparisons: **$p < .01$; n.s., not significant

in widespread brain regions[39] or interact with normal brain networks to disrupt specific functions, such as memory.[40]

Importantly, we showed that phase-locking was consistent across IED types (and thus patients) and involved mainly the ipsilateral frontal cortex, insula, and

ipsilateral and contralateral lateral temporal regions (Figure S6). The involvement of the insula and prefrontal cortex resonates with the concept of temporoperisylvian epilepsy,[41] whereas lateral temporal cortices are known to connect to the hippocampal formation.[42] Thus, rather than a blind and diffuse phase-locking, current evidence suggests a set of specific brain regions that account for extra-IZ phase-locking and presumably constitute an epileptic network. However, it remains puzzling why the extra-IZ phase-locking is more systematically found across the three filtering methods than locking to intra-IZ oscillations. Further abnormalities of neural activity may be more pronounced within the IZ and interfere with the signal-to-noise ratio when assessing phase-locking inside the IZ. A complementary view could be that the IZ exhibits abnormal activity already at baseline and thereby fails in precisely locking IEDs to ongoing oscillations that are entrained by the joint effect from relevant regions outside the IZ.[43] Given that SOs depend on the interaction between cortical and thalamic oscillators,[44] the thalamus could play a pivotal role in the emergence of these vulnerable windows.

4.3 | Increase in phase–amplitude coupling: A critical mechanism in emergence of IEDs

IEDs occur during periodic phase angles that represent recurrent transient permissive windows for their expression. The widespread pattern of this permissive activity and the spatial selectivity of the coupling between neuronal discharges and SOs are coherent from a biological perspective; the phase of an oscillation can modulate the activity of distant brain regions, whereas the neural activity eventually recruited in a given task is spatially specific,[45] including instances of pathological activity.[9] Although significant, the pre-IED increase in phase–amplitude coupling inside the IZ can appear small at first sight (interquartile range of .1%–4.1% across the 10 patients). Nevertheless, its significance is meaningful, as it should not be expected that all neurons contribute equally to generating IEDs.[19,20] Some neurons even show a decreased firing during IEDs.[19,20] The small effect in our study could thus represent the macroscopic measurable tip of the iceberg of firing disbalance leading to IEDs.

Previous publications have shown that phase–amplitude coupling evolves along the duration of epileptic seizures.[46] It can also help to identify the SOZ,[14–17] to differentiate ictal from interictal high-frequency oscillations,[47] and to predict upcoming seizures.[34] Our findings thus fit nicely with the hypothesis that phase–amplitude coupling, by modifying the coordination of neuronal firing, could support the expression of pathological epileptic transients. Perturbation in the coupling between SOs (<1.25 Hz) and sleep spindles has been implicated in impaired memory consolidation associated with aging.[48] In future studies, it would thus be interesting to assess whether such a disrupted coupling (between SOs and spindles and/or neuronal discharges) is also involved in memory deficits frequently seen in patients with temporal lobe epilepsy.[49]

4.4 | Methodological considerations and limitations

IEDs are known to occur preferentially during slow waves of sleep, and more specifically at the transition from the up to the down state.[11] As our dataset is made predominantly of awake resting-state recordings (as assessed by concurrent scalp channels), it is highly probable that IEDs are not strictly associated with slow waves of sleep, but with local increase of SOs in general. We unfortunately do not have sufficient sleep data to make reliable inferences on the comparison between SOs during wake and different sleep stages.

We acknowledge that our sample size is limited. Through this proof-of-concept study, we wanted to establish precise changes in ongoing rhythms directly before IEDs, which was possible in raw averages (Figure 1) and even in a single trial (Figure 2). Epileptic discharges follow a multidien pattern of occurrence,[13] but it remains unknown whether changes in specific neuronal patterns precede them on a much shorter timescale. Increasing the sample size would certainly help to validate our results, but above all, it could reveal whether certain subgroups of focal epilepsy (defined by SOZ location, pathological etiology, pharmacoresistance, or other characteristics) do not show such interaction with SOs, a question that lies beyond the scope of our study.

The different filtering methods yielded different results for some analysis. This is most probably due to the IEDs affecting differentially the preceding window of analysis, depending on the filter choice. In the classical method ("filtfilt"), the IEDs can leak over the window of analysis, affecting the amplitude and phase of the signal. In the forward method ("filter"), the IEDs does not leak, but the filter can lead to a phase distortion. In the inverted method ("filtfilt + inversion of the signal"), there is neither leakage of the IED (as it has been suppressed by construction) nor phase distortion. Last, it is possible that false oscillations[25] affected the pre-IED window and introduced nonsystematic bias, as all IEDs are obviously not strictly identical. The strength of our work was precisely to use

three complementary filtering approaches, as well as to stop the time window for statistical analysis well before the statistical onset of IEDs. Using these precautions, we were able to draw reliable conclusions on the interaction between SOs and IEDs, and to dissect the dynamics that anticipate IEDs.

Further limitations are discussed in the Supporting Information.

4.5 | Conclusions and perspectives

Decoding the pathological rhythms underlying the emergence of epileptic activities remains challenging, yet the ability to recognize and anticipate IEDs opens the perspective of new treatments, and in particular the ability to modulate disease activity with neuroresponsive devices. Closed-loop neuromodulation devices are effective in animal models of epilepsy,[32,37,38] but the prediction of IEDs or seizures in humans remains highly challenging.[12,50] Our work identifies complex changes in slow oscillatory activity preceding the emergence of IEDs and could thus open avenues for predictive detection and therapeutic interventions.

CONFLICT OF INTEREST
S.V. and M.S. are advisors and shareholders of Epilog. None of the other authors has any conflict of interest to disclose. We confirm that we have read the Journal's position on issues involved in ethical publication and affirm that this report is consistent with those guidelines.

AUTHOR CONTRIBUTIONS
Laurent Sheybani: Conception and design of the study, analysis of data, drafting a significant portion of the manuscript and figures. Pierre Mégevand: Acquisition and analysis of data, drafting a significant portion of the manuscript and figures. Laurent Spinelli: Acquisition and analysis of data. Christian G. Bénar: Analysis of data, drafting a significant portion of the manuscript. Shahan Momjian: Acquisition and analysis of data. Margitta Seeck: Acquisition and analysis of data. Charles Quairiaux: Analysis of data. Andreas Kleinschmidt: Conception and design of the study, analysis of data, drafting a significant portion of the manuscript. Serge Vulliémoz: Conception and design of the study, acquisition and analysis of data, drafting a significant portion of the manuscript and figures.

ORCID
Laurent Sheybani https://orcid.org/0000-0003-4824-6408
Pierre Mégevand https://orcid.org/0000-0002-0427-547X
Charles Quairiaux https://orcid.org/0000-0003-3770-8232
Serge Vulliémoz https://orcid.org/0000-0002-1877-8625

REFERENCES
1. Pillai J, Sperling MR. Interictal EEG and the diagnosis of epilepsy. Epilepsia. 2006;47(Suppl 1):14–22.
2. Megevand P, Spinelli L, Genetti M, Brodbeck V, Momjian S, Schaller K, et al. Electric source imaging of interictal activity accurately localises the seizure onset zone. J Neurol Neurosurg Psychiatry. 2014;85(1):38–43.
3. Staley KJ, Dudek FE. Interictal spikes and epileptogenesis. Epilepsy Curr. 2006;6(6):199–202.
4. Avoli M, Biagini G, De Curtis M. Do interictal spikes sustain seizures and epileptogenesis? Epilepsy Curr. 2006;6(6):203–7.
5. Kleen JK, Scott RC, Holmes GL, Roberts DW, Rundle MM, Testorf M, et al. Hippocampal interictal epileptiform activity disrupts cognition in humans. Neurology. 2013;81(1):18–24.
6. Cohen I, Navarro V, Clemenceau S, Baulac M, Miles R. On the origin of interictal activity in human temporal lobe epilepsy in vitro. Science. 2002;298(5597):1418–21.
7. Fries P. A mechanism for cognitive dynamics: neuronal communication through neuronal coherence. Trends Cogn Sci. 2005;9(10):474–80.
8. Sadaghiani S, Kleinschmidt A. Brain networks and α-oscillations: structural and functional foundations of cognitive control. Trends Cogn Sci. 2016;20(11):805–17.
9. Sheybani L, van Mierlo P, Birot G, Michel CM, Quairiaux C. Large-scale 3–5 Hz oscillation constrains the expression of neocortical fast ripples in a mouse model of mesial temporal lobe epilepsy. Eneuro. 2019;6(1):ENEURO.0494-18.2019.
10. Nir Y, Staba RJ, Andrillon T, Vyazovskiy VV, Cirelli C, Fried I, et al. Regional slow waves and spindles in human sleep. Neuron. 2011;70(1):153–69.
11. Frauscher B, von Ellenrieder N, Ferrari-Marinho T, Avoli M, Dubeau F, Gotman J. Facilitation of epileptic activity during sleep is mediated by high amplitude slow waves. Brain. 2015;138(6):1629–41.
12. Stirling RE, Cook MJ, Grayden DB, Karoly PJ. Seizure forecasting and cyclic control of seizures. Epilepsia. 2021;62(Suppl 1):S2–14.
13. Baud MO, Kleen JK, Mirro EA, Andrechak JC, King-Stephens D, Chang EF, et al. Multi-day rhythms modulate seizure risk in epilepsy. Nat Commun. 2018;9(1):88.
14. Ibrahim GM, Wong SM, Anderson RA, Singh-Cadieux G, Akiyama T, Ochi A, et al. Dynamic modulation of epileptic high frequency oscillations by the phase of slower cortical rhythms. Exp Neurol. 2014;251:30–8.
15. Weiss SA, Banks GP, McKhann GM, Goodman RR, Emerson RG, Trevelyan AJ, et al. Ictal high frequency oscillations distinguish two types of seizure territories in humans. Brain. 2013;136(12):3796–808.

16. Samiee S, Lévesque M, Avoli M, Baillet S. Phase-amplitude coupling and epileptogenesis in an animal model of mesial temporal lobe epilepsy. Neurobiol Dis. 2018;114:111–9.

17. Amiri M, Frauscher B, Gotman J. Interictal coupling of HFOs and slow oscillations predicts the seizure-onset pattern in mesiotemporal lobe epilepsy. Epilepsia. 2019;60(6):1160–1170.

18. Ren L, Kucewicz MT, Cimbalnik J, Matsumoto JY, Brinkmann BH, Hu W, et al. Gamma oscillations precede interictal epileptiform spikes in the seizure onset zone. Neurology. 2015;84(6):602–8.

19. Keller CJ, Truccolo W, Gale JT, Eskandar E, Thesen T, Carlson C, et al. Heterogeneous neuronal firing patterns during interictal epileptiform discharges in the human cortex. Brain. 2010;133(6):1668–81.

20. Alvarado-Rojas C, Lehongre K, Bagdasaryan J, Bragin A, Staba R, Engel J, et al. Single-unit activities during epileptic discharges in the human hippocampal formation. Front Computat Neurosci. 2013;7:140.

21. Ray S, Crone NE, Niebur E, Franaszczuk PJ, Hsiao SS. Neural correlates of high-gamma oscillations (60–200 Hz) in macaque local field potentials and their potential implications in electrocorticography. J Neurosci. 2008;28(45):11526–36.

22. Brunet D, Murray MM, Michel CM. Spatiotemporal analysis of multichannel EEG: CARTOOL. Comput Intell Neurosci. 2011;2011:1–15.

23. Kural MA, Duez L, Sejer Hansen V, Larsson PG, Rampp S, Schulz R, et al. Criteria for defining interictal epileptiform discharges in EEG: a clinical validation study. Neurology. 2020;94(20):e2139–47.

24. Heers M, Helias M, Hedrich T, Dümpelmann M, Schulze-Bonhage A, Ball T. Spectral bandwidth of interictal fast epileptic activity characterizes the seizure onset zone. Neuroimage Clin. 2018;17:865–72.

25. Bénar C, Chauvière L, Bartolomei F, Wendling F. Pitfalls of high-pass filtering for detecting epileptic oscillations—a technical note on « false » ripples.pdf. Clin Neurophysiol. 2010;121:301–10.

26. Sheybani L, Birot G, Contestabile A, Seeck M, Kiss JZ, Schaller K, et al. Electrophysiological evidence for the development of a self-sustained large-scale epileptic network in the kainate mouse model of temporal lobe epilepsy. J Neurosci. 2018;38(15):3776–91.

27. Vyazovskiy VV, Olcese U, Hanlon EC, Nir Y, Cirelli C, Tononi G. Local sleep in awake rats. Nature. 2011;472(7344):443–7.

28. Mazaheri A, Jensen O. Posterior α activity is not phase-reset by visual stimuli. Proc Natl Acad Sci U S A. 2006;103(8):2948–52.

29. Berens P. CircStat: a MATLAB toolbox for circular statistics. J Stat Softw. 2009;31(10):1–21.

30. Tort ABL, Komorowski RW, Manns JR, Kopell NJ, Eichenbaum H. Theta-gamma coupling increases during the learning of item-context associations. Proc Natl Acad Sci U S A. 2009;106(49):20942–7.

31. Oostenveld R, Fries P, Maris E, Schoffelen J-M. FieldTrip: open source software for advanced analysis of MEG, EEG, and invasive electrophysiological data. Comput Intell Neurosci. 2011;2011:1–9.

32. Berenyi A, Belluscio M, Mao D, Buzsaki G. Closed-loop control of epilepsy by transcranial electrical stimulation. Science. 2012;337(6095):735–7.

33. Thézé R, Giraud A-L, Mégevand P. The phase of cortical oscillations determines the perceptual fate of visual cues in naturalistic audiovisual speech. Sci Adv. 2020;6(45):eabc6348.

34. Alvarado-Rojas C, Valderrama M, Fouad-Ahmed A, Feldwisch-Drentrup H, Ihle M, Teixeira CA, et al. Slow modulations of high-frequency activity (40–140 Hz) discriminate preictal changes in human focal epilepsy. Sci Rep. 2015;4(1):4545.

35. Richardson MP. Large scale brain models of epilepsy: dynamics meets connectomics. J Neurol Neurosurg Psychiatry. 2012;83(12):1238–48.

36. Aubert S, Wendling F, Regis J, McGonigal A, Figarella-Branger D, Peragut J-C, et al. Local and remote epileptogenicity in focal cortical dysplasias and neurodevelopmental tumours. Brain. 2009;132(11):3072–86.

37. Krook-Magnuson E, Armstrong C, Oijala M, Soltesz I. On-demand optogenetic control of spontaneous seizures in temporal lobe epilepsy. Nat Commun. 2013;4:1376.

38. Paz JT, Davidson TJ, Frechette ES, Delord B, Parada I, Peng K, et al. Closed-loop optogenetic control of thalamus as a tool for interrupting seizures after cortical injury. Nat Neurosci. 2013;16(1):64–70.

39. Dahal P, Ghani N, Flinker A, Dugan P, Friedman D, Doyle W, et al. Interictal epileptiform discharges shape large-scale intercortical communication. Brain. 2019;142(11):3502–13.

40. Gelinas JN, Khodagholy D, Thesen T, Devinsky O, Buzsáki G. Interictal epileptiform discharges induce hippocampal–cortical coupling in temporal lobe epilepsy. Nat Med. 2016;22(6):641–8.

41. Bartolomei F, Cosandier-Rimele D, McGonigal A, Aubert S, Régis J, Gavaret M, et al. From mesial temporal lobe to temporoperisylvian seizures: a quantified study of temporal lobe seizure networks. Epilepsia. 2010;51(10):2147–58.

42. Mégevand P, Groppe DM, Bickel S, Mercier MR, Goldfinger MS, Keller CJ, et al. The hippocampus and amygdala are integrators of neocortical influence: a corticocortical evoked potential study. Brain Connect. 2017;7(10):648–60.

43. D'Alessandro M, Esteller R, Vachtsevanos G, Hinson A, Echauz J, Litt B. Epileptic seizure prediction using hybrid feature selection over multiple intracranial EEG electrode contacts: a report of four patients. IEEE Trans Biomed Eng. 2003;50(5):603–15.

44. Crunelli V, Hughes SW. The slow (<1 Hz) rhythm of non-REM sleep: a dialogue between three cardinal oscillators. Nat Neurosci. 2010;13(1):9.

45. Fujisawa S, Buzsáki G. A 4 Hz oscillation adaptively synchronizes prefrontal, VTA, and hippocampal activities. Neuron. 2011;72(1):153–65.

46. Zhang R, Ren Y, Liu C, Xu N, Li X, Cong F, et al. Temporal-spatial characteristics of phase-amplitude coupling in electrocorticogram for human temporal lobe epilepsy. Clin Neurophysiol. 2017;128(9):1707–18.

47. Nariai H, Matsuzaki N, Juhász C, Nagasawa T, Sood S, Chugani HT, et al. Ictal high-frequency oscillations at 80–200 Hz coupled with delta phase in epileptic spasms. Epilepsia. 2011;52(10):e130–4.

48. Helfrich RF, Mander BA, Jagust WJ, Knight RT, Walker MP. Old brains come uncoupled in sleep: slow wave-spindle synchrony, brain atrophy, and forgetting. Neuron. 2018;97(1):221–30.e4.

49. Helmstaedter C, Kockelmann E. Cognitive outcomes in patients with chronic temporal lobe epilepsy. Epilepsia. 2006;47(Suppl 2):96–8.

50. Bernard C. Circadian/multidien molecular oscillations and rhythmicity of epilepsy (MORE). Epilepsia. 2021;62(Suppl 1):S49–68.

SUPPORTING INFORMATION

Additional supporting information may be found online in the Supporting Information section.